

## Alford rotation, ray theory, and crossed-dipole geometry

Joe A. Dellinger\*, Bertram Nolte<sup>†</sup>, and John T. Etgen\*

### ABSTRACT

Two generalizations of Alford rotation have been proposed for processing  $2 \times 2$ -component data containing nonorthogonal split shear waves: singular value decomposition (SVD) and eigenvector-eigenvalue decomposition (EED). Using a simple crossed-dipole synthetic model, we demonstrate that the physical model behind the EED method is invalid. It incorrectly assumes that a vector source aligned with the particle motion of an anisotropic pure mode will excite only that one mode. Ray theory shows that a vector point-force source embedded in a homogeneous anisotropic medium instead excites all those modes with particle motions that are not perpendicular to the direction of the applied force, just as a vector point receiver detects all modes with polarizations that are not perpendicular to the receiver. Correctly generalized Alford rotation synthesizes vector sources and receivers such that each component is perpendicular to all but one of the pure modes of the medium.

Although this ray-theory result does not allow for the possibility of a source or receiver on a free surface and so is not yet completely general, it does apply to the idealized homogeneous crossed-dipole geometry of our example. The new method, symmetric Alford diagonalization, differs from previous methods by becoming unstable when applied over excessively short time windows. This behavior is consistent with the physics of the problem: If nonorthogonal modes are allowed, then there is not enough information at a single time sample to determine a unique solution. Any method that can find a unique solution at a single time sample, including both the EED and SVD methods, does not respect the physics of the nonorthogonal problem. Although there appears to be no problem that recommends the EED method over standard Alford rotation for its solution, the SVD method is still applicable to the problem it was originally designed to solve: orthogonal modes with an unknown source or receiver orientation.

### INTRODUCTION

Alford rotation is a widely used technique for separating split shear waves in  $2 \times 2$ -component seismic data (Alford, 1986, 1989; Thomsen, 1988). By  $2 \times 2$ -component (henceforth  $2 \times 2$ -C) we mean  $X$  and  $Y$  sources shot into  $X$  and  $Y$  receivers. The seismogram components of the  $2 \times 2$  data matrix are individually denoted  $XX$ ,  $XY$ ,  $YX$ , and  $YY$ , with the source polarization given by the first letter and the receiver polarization by the second. (This  $2 \times 2$ -C recording geometry has traditionally been called 4C, but that older definition of 4C has been supplanted by the modern ocean-bottom-seismic one of a pressure source shot into  $X$ ,  $Y$ ,  $Z$ , and pressure receivers.) Alford rotation was originally used for processing  $2 \times 2$ -C surface seismic and VSP data. More recently it has come to be used for processing  $2 \times 2$ -C crossed-dipole data as

well (Esmersoy et al., 1994; Koster et al., 1994; Mueller et al., 1994).

Alford rotation separates the pure-mode waves by mathematically rotating the sources and receivers into alignment with the natural coordinate system of the anisotropic earth. Ideally, the rotated  $X'X'$  trace should then contain one of the two pure shear modes, the  $Y'Y'$  trace the other, and the off-diagonal  $X'Y'$  and  $Y'X'$  traces only noise. In practice the rotation angle is not known, and a search is made to find the angle that comes closest to diagonalizing the data. The angle could also be determined analytically (Murtha, 1988; Winterstein, 1992).

Alford rotation was originally derived from a consideration of the physics of elastic plane waves vertically propagating in a stratified orthorhombically anisotropic medium (Alford, 1986). Although the magnitude of the anisotropy may vary with depth, one of the three principal axes of the orthorhombic

Includes material presented at the 66th and 68th Annual International Meetings, Society of Exploration Geophysicists. Manuscript received by the Editor March 2, 1999; revised manuscript received June 26, 2000. Published on Geophysics Online August 24, 2000.

\*BP Amoco, 200 Westlake Park Blvd., Houston, Texas, 77079. E-mail: dellinja@bp.com; jetgen@amoco.com.

†Formerly Texaco Upstream Technology, 4800 Fournace Place, BOB-W571, Bellaire, Texas 77401; presently BP Amoco, 200 Westlake Park Blvd., Houston, Texas, 77079.

© 2001 Society of Exploration Geophysicists. All rights reserved.

anisotropy (presumably controlled by gravity) must always be vertical, and the azimuths of the two horizontal principal axes (presumably controlled by a regional stress field) must be the same for all depths. Because it respects the physics of this model, Alford rotation implicitly assumes there are exactly two mutually orthogonal shear waves independently propagating from source to receiver (Auld, 1973). Standard Alford rotation also assumes that the sources and receivers are mutually orthogonal and aligned. Because the vertical axis is a symmetry axis of the orthorhombic anisotropy in this model, Alford rotation remains valid if the vertically propagating plane waves are replaced with vertically propagating rays (Auld, 1973; Thomsen, 1988).

Several generalizations of standard Alford rotation have been proposed. Layer stripping allows the horizontal principal axes to vary in azimuth with depth, so that the modes no longer propagate independently but couple at the layer interfaces (Winterstein and Meadows, 1991; Thomsen et al., 1999). Layer stripping should similarly allow any general diagonalization technique designed for homogeneous media (i.e., ones with no conversion between the pure modes at layer boundaries) to be extended to layered media.

The two other widely used generalizations of standard Alford rotation correspond to well-known matrix-decomposition techniques applied to the  $2 \times 2$ -C data matrix (see, e.g., Golub and Van Loan, 1983). The first of these calculates its singular value decomposition (SVD). This method has the same underlying model as standard Alford rotation but relaxes the assumption that the sources and receivers are specified in the same coordinate system, allowing them to rotate independently. The SVD method is typically used in situations where there is an unknown misalignment between the orientations of the sources and receivers that must be determined from the data (Alford, 1991; MacBeth and Crampin, 1991; Zeng and MacBeth, 1993; MacBeth et al., 1994).

The second technique is eigenvector-eigenvalue decomposition (EED) of the  $2 \times 2$ -C data matrix. This method was proposed as a way to relax the orthogonality assumption of standard Alford rotation, allowing diagonalization of a data matrix that is nonsymmetric because of nonorthogonal split shear modes (Li and Crampin, 1993). For the traditional zero-offset surface-seismic case, this is perhaps not a very useful generalization; in the absence of complex geological structure, the waves would predominantly travel vertically—a direction quite likely to lie in a symmetry plane of the anisotropic earth—and the shear waves would then be orthogonal (Auld, 1973). However, this unusually symmetric special case is much less likely to happen for a crossed-dipole survey logged in a non-vertical borehole. A method that can (correctly) diagonalize nonorthogonal split shear modes might prove useful for processing crossed-dipole data.

Although the EED method has appeared in the literature (Li and Crampin, 1993; Zeng and MacBeth, 1993; MacBeth and Li, 1996; Li et al., 1998) as an application of the linear transform technique (LTT) introduced by Li and Crampin (1993), the LTT transform itself is rather general and can be used to diagonalize the  $2 \times 2$ -C data matrix in any of several different ways. If the data matrix is symmetric, the LTT transform provides an alternative method for performing standard Alford rotation and for directly determining the optimal Alford rotation angle.

Either of these methods, SVD or EED, can be used to diagonalize arbitrary  $2 \times 2$  data matrices, something standard Alford rotation cannot do. In the absence of physical insight, however, there is no reason to expect that the diagonalized time series produced by any of these methods should be physically meaningful. Dellinger and Nolte (1996, 1997) demonstrate that physically meaningless diagonalizations can happen using a simple thought experiment, a multicomponent source and receiver embedded in an infinite homogeneous (but generally anisotropic) whole space. Because of the general anisotropy, the true pure modes propagating along the ray from source to receiver in this model are not generally orthogonal (see, e.g., Li et al., 1998). Even so, this idealized homogeneous crossed-dipole geometry always produces a symmetric  $2 \times 2$ -C data matrix, regardless of the anisotropy. All three diagonalization methods in common use (standard Alford, SVD, and EED) will exactly model symmetric data as a superposition of (possibly time-varying) orthogonal pure modes. For this simple homogeneous example, however, these derived orthogonal modes generally will not correspond to the true nonorthogonal modes of the model.

By appealing to the principle of seismic reciprocity (Knopoff and Gangi, 1959), Dellinger et al. (1998) proposed a new diagonalization equation for use in this geometry. We begin by reviewing the background and conclusions of the crossed-dipole thought experiment of Dellinger and Nolte (1996, 1997) and then go on to verify their predictions using a synthetic data set. As expected, the proposed equation correctly diagonalizes this data set. We also demonstrate that it can be used for solving for the unknown pure modes in homogeneous crossed-dipole data in a way exactly analogous with standard Alford rotation. The new method, symmetric Alford diagonalization, is very similar to the EED method in form (and we will also make use of the LTT transform in implementing it) but differs significantly in its properties. We conclude by discussing the theoretical implications of the result—in particular, by showing its relationship to a well-known equation in ray theory (Buchwald, 1959; Lighthill, 1960; Burridge, 1967; Hanyga, 1984; Ben-Menahem and Sena, 1990; Tsvankin and Chesnokov, 1990; Gajewski, 1993; Pšenčík and Teles, 1996).

### THE GENERAL LINEAR MODEL

All three diagonalization methods currently in use (standard Alford, SVD, and EED) share a common mathematical model, the general linear modeling equation:

$$\mathbf{R} = \begin{pmatrix} R_{XX} & R_{YX} \\ R_{XY} & R_{YY} \end{pmatrix} = \mathbf{P}_{M \rightarrow R} \mathbf{D} \mathbf{P}_{S \rightarrow M} \mathbf{S}, \quad (1)$$

where  $\mathbf{S}$ , an identity matrix, defines the  $X$  and  $Y$  sources,  $\mathbf{P}_{S \rightarrow M}$  decomposes the source vectors into a sum of pure modes, the diagonal matrix  $\mathbf{D}$  extrapolates the pure modes from source to receiver,  $\mathbf{P}_{M \rightarrow R}$  projects the pure modes onto the  $X$  and  $Y$  receiver components and sums, and  $\mathbf{R}$  is the recorded  $2 \times 2$ -C data matrix. (Note  $R$  for receiver,  $S$  for source,  $D$  for diagonal,  $P$  for projection, and  $M$  for mode.) Any modeling equation assuming linearity and the existence of independently propagating pure modes must have this form (Zeng and MacBeth, 1993).

Equation (1) is easily rearranged to give  $\mathbf{D}$  in terms of the recorded data matrix  $\mathbf{R}$ , yielding the general linear processing

equation:

$$\mathbf{P}_{M \rightarrow R}^{-1} \mathbf{R} \mathbf{P}_{S \rightarrow M}^{-1} = \mathbf{D} = \begin{pmatrix} D_{11} & D_{12} \\ D_{21} & D_{22} \end{pmatrix}. \quad (2)$$

Ideally, the pure-mode matrix  $\mathbf{D}$  produced by applying this equation to real data should be diagonal, with distinct pure-mode data sets in the diagonal elements  $D_{11}$  and  $D_{22}$  and only noise in the off-diagonal elements  $D_{12}$  and  $D_{21}$ .

For the case of standard Alford rotation, the orthogonal shear waves of the medium define a natural coordinate system. The projection matrix  $\mathbf{P}_{S \rightarrow M}$  rotates into this natural coordinate system, and the projection matrix  $\mathbf{P}_{M \rightarrow R}$  rotates back out again (Thomsen, 1988). Mathematically, we have

$$\mathbf{P}_{S \rightarrow M} = \begin{pmatrix} \cos \theta_S & -\sin \theta_S \\ \sin \theta_S & \cos \theta_S \end{pmatrix}^T \quad (3)$$

and

$$\mathbf{P}_{M \rightarrow R} = \begin{pmatrix} \cos \theta_R & -\sin \theta_R \\ \sin \theta_R & \cos \theta_R \end{pmatrix}, \quad (4)$$

with  $\theta_S = \theta_R$  (Thomsen, 1988). If the sources and receivers are not mutually aligned, there is no reason to expect  $\theta_S = \theta_R$ . By dropping this restriction we obtain the SVD generalization of standard Alford rotation (Alford, 1991; MacBeth and Crampin, 1991; MacBeth et al., 1994). (Note different authors have their own names for this method.) For the SVD method to produce a physically meaningful diagonalization, the background medium should conform to the traditional Alford model of orthogonal pure shear modes and unvarying principal directions.

### The EED method

Alford rotation was derived from consideration of plane-wave propagation (Alford, 1986). Most seismic experiments are better approximated by propagation along rays. For a given ray direction there will be two (or more) possible quasi-shear-wave particle-motion polarizations. If the ray is not propagating in a symmetry plane, the polarizations of these waves generally are not orthogonal.

For the case of standard Alford rotation (with  $\theta_S = \theta_R$ ), we have both

$$\mathbf{P}_{S \rightarrow M} = \mathbf{P}_{M \rightarrow R}^{-1} \quad (5)$$

and

$$\mathbf{P}_{S \rightarrow M} = \mathbf{P}_{M \rightarrow R}^T. \quad (6)$$

Li and Crampin (1993) propose generalizing standard Alford rotation to handle nonorthogonal modes by using equations (1), (2), and (5) exactly as in Alford rotation but without the restriction that  $\mathbf{P}_{M \rightarrow R}$  must be a rotation matrix [given by also requiring equation (6)]. The matrix  $\mathbf{P}_{S \rightarrow M}$  then transforms the source components into the natural nonorthogonal coordinate system of the anisotropy, and the matrix  $\mathbf{P}_{M \rightarrow R} = \mathbf{P}_{S \rightarrow M}^{-1}$  transforms back. When used to process data, this method calculates the eigenvector-eigenvalue decomposition of the square data matrix  $\mathbf{R}$  (see, e.g., Golub and Van Loan, 1983), which is why we call it the EED method.

The EED modeling equation is

$$\mathbf{R} = \mathbf{P}_{M \rightarrow R} \mathbf{D} \mathbf{P}_{M \rightarrow R}^{-1}, \quad (7)$$

where

$$\mathbf{P}_{M \rightarrow R} = \begin{pmatrix} \cos \theta_1 & \cos \theta_2 \\ \sin \theta_1 & \sin \theta_2 \end{pmatrix}. \quad (8)$$

The azimuths of the two split shear modes are given by  $\theta_1$  and  $\theta_2$ , both measured from, e.g., the  $X$ -axis. [Compare equation (7) with equation (26b) in MacBeth and Li (1996) and (after setting  $\alpha_G = 0$ ) equation (14) in Li et al. (1998).]

Figure 1 shows how the EED modeling equation would apply to the problem of a source in a medium with one pure mode aligned with the  $X$ -axis and the other making an angle of  $45^\circ$  to the first. A unit  $X$  source excites a unit magnitude of the first mode; a unit  $Y$  source is composed of a magnitude of  $-1$  of the first mode and a magnitude of  $+\sqrt{2}$  of the second. The diagonal matrix  $\mathbf{D}$  in the EED modeling equation (7) then splits the arrival times of the two pure modes so they arrive at the receivers separately. When the first pure mode (with pure  $X$  polarization) arrives, it excites only the  $X$  receiver; the  $XY$  component of  $\mathbf{R}$  is therefore zero. When the second pure mode (a mixture of  $X$  and  $Y$ ) arrives, however, it excites both the  $X$  and  $Y$  receivers; the  $YX$  component of  $\mathbf{R}$  is therefore nonzero. Mathematically, we have

$$\mathbf{R} = \begin{pmatrix} R_{XX} & R_{YX} \neq 0 \\ R_{XY} = 0 & R_{YY} \end{pmatrix} = \begin{pmatrix} 1 & 1/\sqrt{2} \\ 0 & 1/\sqrt{2} \end{pmatrix} \mathbf{D} \begin{pmatrix} 1 & -1 \\ 0 & \sqrt{2} \end{pmatrix}, \quad (9)$$

and  $\mathbf{R}$  is nonsymmetric for this example.

Thus, according to the EED modeling equation, nonorthogonal modes should result in a nonsymmetric data matrix (Li and Crampin, 1993; MacBeth and Li, 1996; Li et al., 1998). As we shall demonstrate, this is a fundamental error. Note also that if the data matrix is symmetric, then  $\mathbf{P}_{M \rightarrow R}^{-1} = \mathbf{P}_{M \rightarrow R}^T$ , the projection matrix  $\mathbf{P}_{M \rightarrow R}^T$  is a rotation, and (according to the EED modeling equation) the modes are orthogonal, just as in standard Alford rotation. Mathematically, this is because the EED method finds for the pure modes the eigenvectors of the data matrix, and real symmetric matrices always have orthogonal eigenvectors (see Golub and Van Loan, 1983).

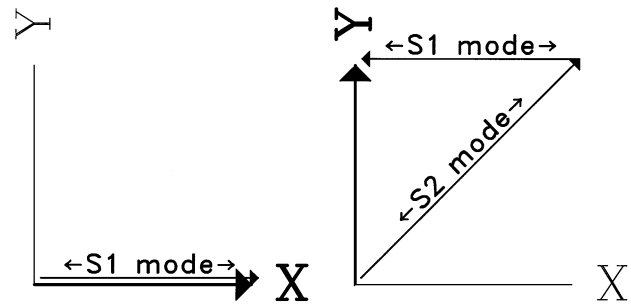


FIG. 1. Decomposition of an  $X$  (left) and  $Y$  (right) source into a sum of nonorthogonal pure modes according to the EED (eigenvector-eigenvalue decomposition) method.

### A SYNTHETIC CROSSED-DIPOLE EXPERIMENT

Dellinger and Nolte (1996, 1997) propose the idealized crossed-dipole geometry as a particularly simple model for testing nonorthogonal decomposition methods. It consists of a multicomponent point source and a multicomponent point receiver some distance away from the source, both embedded in an infinite homogeneous medium. Figure 2 shows a numerical example, calculated using the general-anisotropy reflectivity modeling program ANIVEC<sup>TM</sup> (Mallick and Frazer, 1990). The normalized elastic stiffnesses for the homogeneous background medium are given in Table 1. The result displays the

complete data-matrix symmetry predicted by Dellinger and Nolte (1996, 1997). [The weak shear arrival with linear move-out centered at about 2.9 s and  $-0.9$  km is a non ray-theoretic event—a plane lid (Burrige, 1967).]

Using the elastic constants in Table 1, we calculated the true anisotropic properties of this medium by solving the Kelvin-Christoffel equation (Auld, 1973) for every grid point on a dense spherical mesh of phase (plane-wave) propagation directions, obtaining phase velocities and particle-motion polarizations for each of the three plane-wave pure modes at each grid point. We next used this information to calculate the corresponding group velocities and group propagation directions for

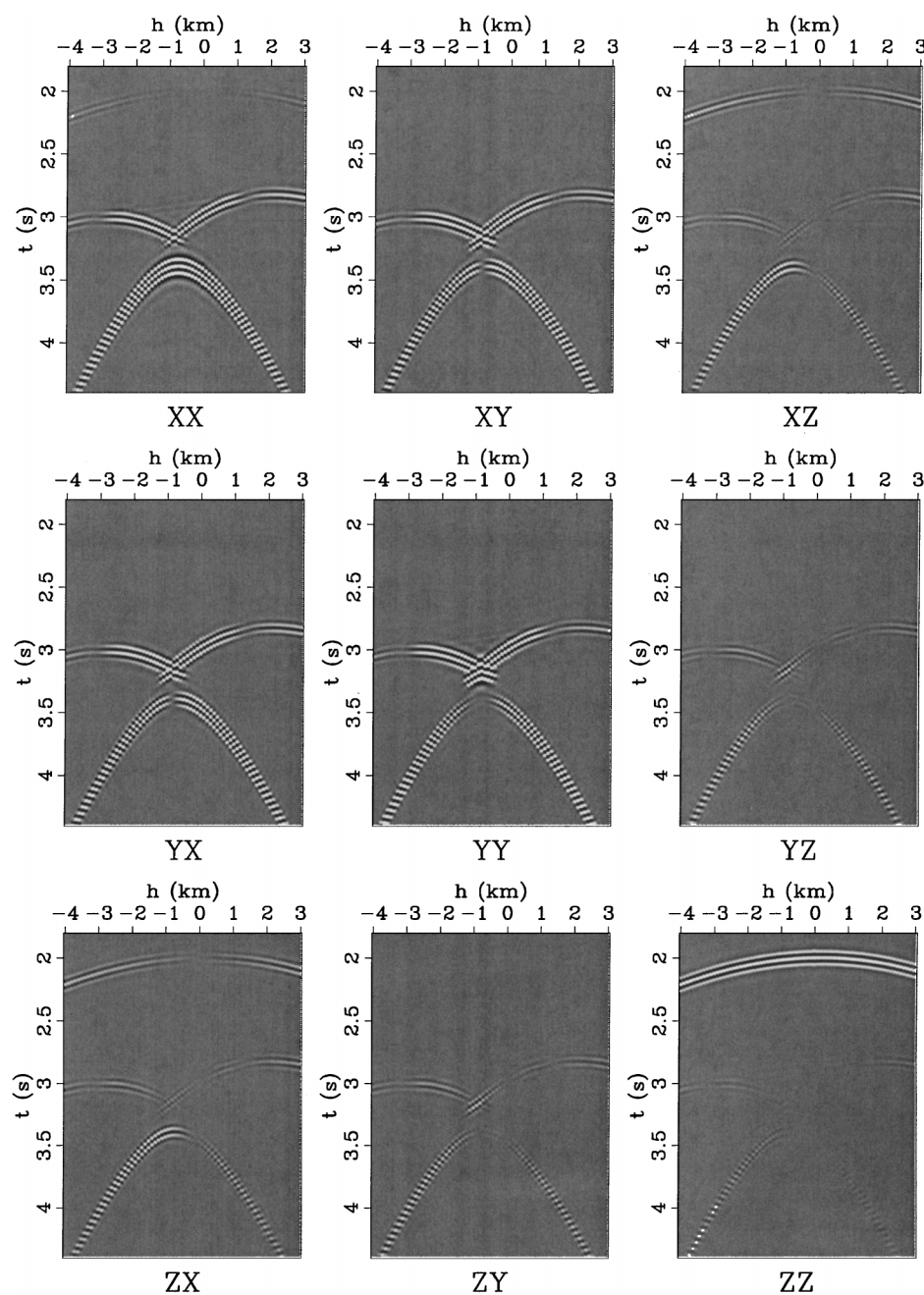


FIG. 2. Nine-component seismograms for a source and receiver embedded in a homogeneous orthorhombic background medium that has been rotated so the Z-axis does not lie in any of the three orthorhombic symmetry planes. The three-component vector source is at location  $(x = 0, y = 0, z = +8 \text{ km})$ , and the three-component vector receivers are at locations  $(x = h, y = 0, z = 0)$ , where  $h$  varies from  $-4$  to  $+3$  km. The data matrix is symmetric:  $XY = YX$ ,  $XZ = ZX$ , and  $YZ = ZY$  for all offsets.

each mode (Winterstein, 1990). By searching over the mesh and refining it as necessary, we then found all the ray-theoretical arrivals, including their group velocities and particle-motion polarizations, for all group (ray) propagation directions of interest. Although the particle motions of the three plane-wave pure modes are always orthogonal for any given phase propagation direction (Auld, 1973), for any given group propagation direction the polarizations of the different arrivals need not be orthogonal; in anisotropic media, the different arrivals generally have different phase propagation directions.

Figure 3 shows hodograms and wiggle traces for the zero-offset record from the data set shown in Figure 2. These traces avoid the shear-wave triplication centered at about offset  $-0.9$  km, so there are only two (extremely well separated)

ray-theoretic shear-wave arrivals. We calculated that for this trace the  $P$ -wave deviates from purely longitudinal polarization (i.e., particle motion parallel to the group propagation direction) by only  $0.3^\circ$  and the shear waves deviate from purely transverse polarization (i.e., particle motion perpendicular to the group propagation direction) by only  $0.6^\circ$ . The two shear waves deviate from being orthogonal to each other, however, by  $14.4^\circ$  (a nonorthogonality clearly visible in the hodograms). As we have already seen, for symmetric ( $XY = YX$ ) data the EED method would have predicted orthogonal modes.

The  $qS1$  and  $qS2$  arrivals in this example have calculated polarization azimuths of  $129.3^\circ$  and  $24.9^\circ$ , respectively. Figure 4 shows the result of forming linear combinations of the seismograms in Figure 3 to synthesize sources aligned with these

**Table 1. The normalized elastic stiffnesses ( $C_{ij}/\rho$ ) for a rotated orthorhombic medium, in units of  $(\text{km/s})^2$ . This medium was designed for testing nonorthogonal shear-wave decompositions. It has almost perfectly longitudinally polarized  $P$ -waves and transversely polarized shear waves for all propagation directions, but the shear waves are strongly split and (for some group propagation directions) markedly nonorthogonal.**

16.0398	9.30334	-3.01053	7.32306	0.187091	-0.0887023
9.30334	16.0000	3.26742	0	-0.641486	0
-3.01053	3.26742	16.0398	-0.00932298	-0.187091	0.857407
7.32306	0	-0.00932298	6.36847	-0.340491	0.299948
0.187091	-0.641486	-0.187091	-0.340491	10.3656	-4.07418
-0.0887023	0	0.857407	0.299948	-4.07418	3.54618

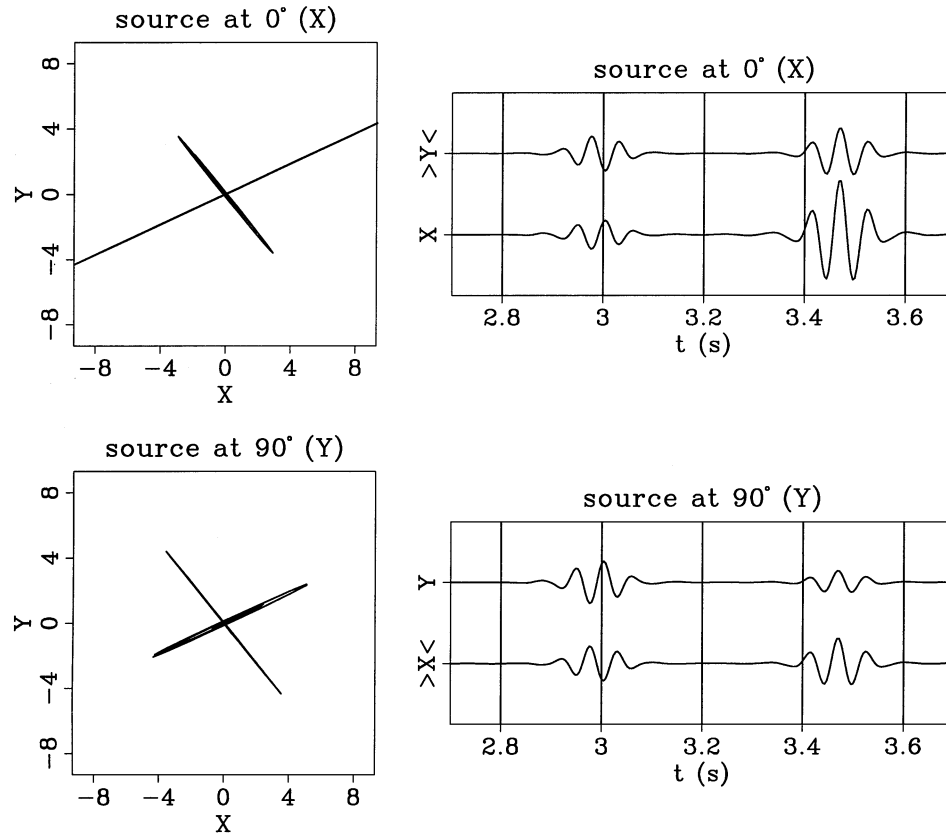


FIG. 3. The zero-offset traces from Figure 2. On the left are the hodograms corresponding to the wiggle traces on the right. The top two plots show the  $X$  and  $Y$  seismograms at the receiver for the  $X$  source. The lower two plots show the corresponding seismograms for the  $Y$  source. Note the  $X$  source into the  $Y$  receiver produces the same seismogram as the  $Y$  source into the  $X$  receiver (the two flagged wiggle traces). The group velocities of the three ray-theoretical arrivals are  $4.004$  km/s (the  $P$ -wave),  $2.675$  km/s ( $qS1$ -wave), and  $2.305$  km/s ( $qS2$ -wave).

two azimuths. According to the source decomposition used by the EED method, rotating the source to align it with a pure mode should only excite that mode [see Appendix B of Li and Crampin (1993)]. This example shows that in fact the other (nonorthogonal) mode is also excited (as standard ray theory would predict; see the discussion below).

### The crossed-dipole modeling equation

Dellinger et al. (1998) note that if we require  $\mathbf{P}_{S \rightarrow M} = \mathbf{P}_{M \rightarrow R}^T$  in the general linear modeling equation (1), the observed symmetry ( $\mathbf{R} = \mathbf{R}^T$ ) is automatically obtained. The modeling equation for the idealized homogeneous crossed-dipole geometry would then be

$$\mathbf{R} = \mathbf{P}_{M \rightarrow R} \mathbf{D} \mathbf{P}_{M \rightarrow R}^T, \quad (10)$$

with no restriction that  $\mathbf{P}_{M \rightarrow R}$  must be a rotation matrix. Without loss of generality, we will require that the columns of  $\mathbf{P}_{M \rightarrow R}$  be normalized.

As we demonstrate in the discussion, equation (10) should be valid for homogeneous media: it is equivalent to a well-known result in the ray-tracing literature, the ray-theoretical vector Green's function due to a vector point force in an infinite homogeneous anisotropic elastic medium (Buchwald, 1959; Lighthill, 1960; Burridge, 1967; Hanyga, 1984; Ben-Menahem and Sena, 1990; Tsvankin and Chesnokov, 1990; Gajewski, 1993; Pšenčík and Teles, 1996). Note that our symmetric

crossed-dipole modeling equation (10) differs from the asymmetric EED modeling equation (7) only by using equation (6) instead of equation (5). All other terms are the same. For orthogonal modes the projection matrices are rotations,  $\mathbf{P}_{M \rightarrow R}^T = \mathbf{P}_{M \rightarrow R}^{-1}$ , and both methods are exactly equivalent to standard Alford rotation.

Equation (10) predicts that a source will excite any mode that it is not perpendicular to. In Figure 5 we test this hypothesis by synthesizing sources perpendicular to the pure modes in our test example. As expected, the perpendicular mode is not excited (barring a tiny residue we believe is the result of numerical noise). If there are only two shear modes (as in this example), it is therefore still possible to excite only one shear mode at a time, but not by aligning the source with the polarization of the desired mode. Instead, the source must be oriented so it is perpendicular to the polarization(s) of the undesired mode(s).

### ALFORD DIAGONALIZATION

Equation (10) can also be rearranged to produce a processing equation:

$$\mathbf{P}_{M \rightarrow R}^{-1} \mathbf{R} (\mathbf{P}_{M \rightarrow R}^{-1})^T = \mathbf{D}, \quad (11)$$

where the unit-magnitude columns of  $\mathbf{P}_{M \rightarrow R}$ , giving the presumed polarizations of the anisotropic pure modes, are chosen to minimize the off-diagonal energy in  $\mathbf{D}$ . We call this method symmetric Alford diagonalization (Dellinger et al.,

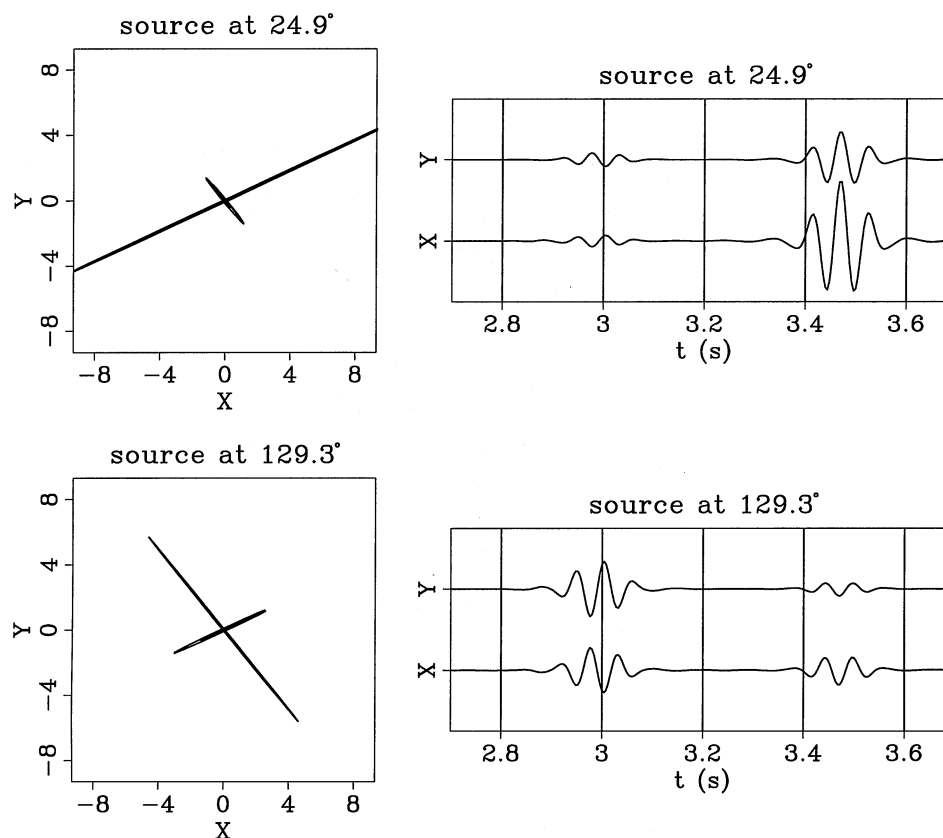


FIG. 4. As Figure 3 but for sources at azimuths of  $24.9^\circ$  and  $129.3^\circ$ , aligned with the predicted polarizations of the split shear modes. Both sources excite both modes.

1998). Equation (11) represents an experiment that could be performed in the field: It diagonalizes the data by synthesizing rotated sources and receivers such that each is orthogonal to a pure mode. If the modes are not orthogonal, the rotated sources (and the rotated receivers) will also not be orthogonal.

We will specify the polarization directions of the pure modes using two angles. The first mode has an angle of  $\theta$ , measured counterclockwise from the  $X$ -axis. The other mode has an angle of  $\theta + \eta$ , measured counterclockwise from the  $Y$ -axis. (If  $\eta = 0$ , the two modes are orthogonal and the method reduces to standard Alford rotation.) We then have

$$\mathbf{P}_{M \rightarrow R} = \begin{pmatrix} \cos(\theta) & -\sin(\theta + \eta) \\ \sin(\theta) & \cos(\theta + \eta) \end{pmatrix} \quad (12)$$

and

$$\mathbf{P}_{M \rightarrow R}^{-1} = \frac{1}{\cos(\eta)} \begin{pmatrix} \cos(\theta + \eta) & \sin(\theta + \eta) \\ -\sin(\theta) & \cos(\theta) \end{pmatrix}. \quad (13)$$

If equation (10) adequately models the problem, then for the correct  $\theta$  and  $\eta$  the pure-mode matrix  $\mathbf{D}$  in equation (11) should become diagonal. This allows us to determine  $\theta$  and  $\eta$  from the recorded data matrix  $\mathbf{R}$ : choose the values that minimize the sum of the squares of the off-diagonal entries of  $\mathbf{D}$ , averaged over some window of the data.

We can express the result compactly by making use of the linear transformations of Li and Crampin (1993). Let

$$\begin{aligned} R_{oa} &= (R_{XY} + R_{YX})/2 \\ R_{da} &= (R_{XX} + R_{YY})/2 \\ R_{os} &= (R_{YX} - R_{XY})/2 \\ R_{ds} &= (R_{YY} - R_{XX})/2 \end{aligned} \quad (14)$$

and

$$\xi = 2\theta + \eta. \quad (15)$$

(Note subscripts  $o$  for off-diagonal,  $d$  for diagonal,  $a$  for add, and  $s$  for subtract.) The result is then

$$\begin{aligned} 0 \approx \langle D_{12}^2 + D_{21}^2 \rangle &= \sec(\eta)^4 (\langle R_{da}^2 \rangle + \langle R_{ds}^2 \rangle + \langle R_{oa}^2 \rangle + \langle R_{os}^2 \rangle \\ &+ (\langle R_{oa}^2 \rangle - \langle R_{ds}^2 \rangle) \cos(2\xi) \\ &+ (\langle R_{os}^2 \rangle - \langle R_{da}^2 \rangle) \cos(2\eta) + 2\langle R_{ds} R_{oa} \rangle \sin(2\xi) \\ &+ 4\langle R_{da} R_{oa} \rangle \cos(\xi) \sin(\eta) \\ &+ 4\langle R_{da} R_{ds} \rangle \sin(\xi) \sin(\eta)), \end{aligned} \quad (16)$$

where quantities inside the angle brackets are averaged over the time window.

If we set  $\eta = 0$ , equation 16 reduces to standard Alford rotation, a problem that is known to always have an exact solution for a symmetric data matrix, time sample by time sample. For a data window only one time sample long, we could also find

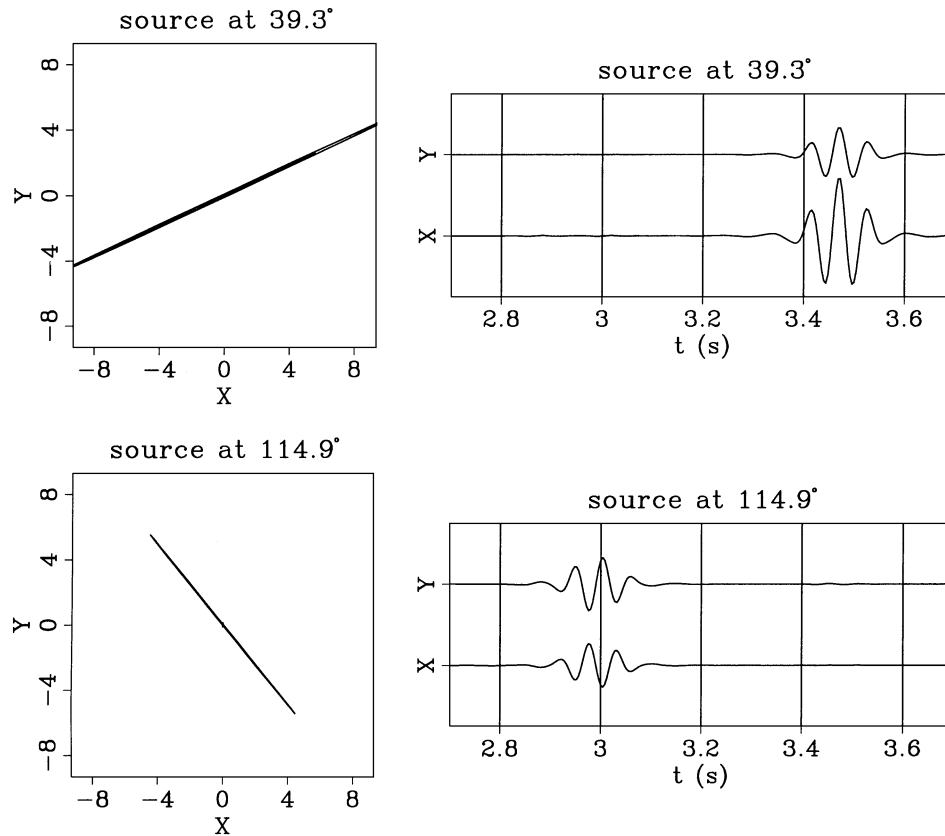


FIG. 5. As Figure 3 but for sources at azimuths of 39.3° and 114.90°, normal to the predicted polarizations of the split shear modes. A pure mode is not excited by a source that is perpendicular to its particle-motion direction.

an exact solution to equation (16) for other values of  $\eta$ . Unlike current methods based on the general linear processing equation (2), our method requires a long enough time window for the split shear waves to vary in relative phase across it to provide an unambiguous result for both  $\theta$  and  $\eta$ .

Figure 6 shows the result of applying equation (16) to the synthetic data shown in Figure 3. The function is well behaved and has a minimum at the expected solution of  $\theta = 24.9^\circ$  and  $\eta = 14.4^\circ$ . (The second minimum at  $\theta = -50.7^\circ$  and  $\eta = -14.4^\circ$  corresponds to exactly the same two shear-wave polarizations as the first.) Figure 7 shows the result of using these angles to perform the diagonalization; the data are diagonalized correctly. Although we chose to demonstrate the method using an example with well separated events, the diagonalization would have worked equally well if the events had overlapped instead. The modes are distinguished by their polarizations, not their arrival times.

Figure 8 shows what happens if the window contains energy almost entirely from only one of the two events; the polarization of the weak event cannot be well determined. If the window contained no energy from the weak event at all, its polarization would be entirely indeterminate. The same ambiguity would also occur for models with overlapping split-shear-wave arrivals if the time window were too short for the distinct iden-

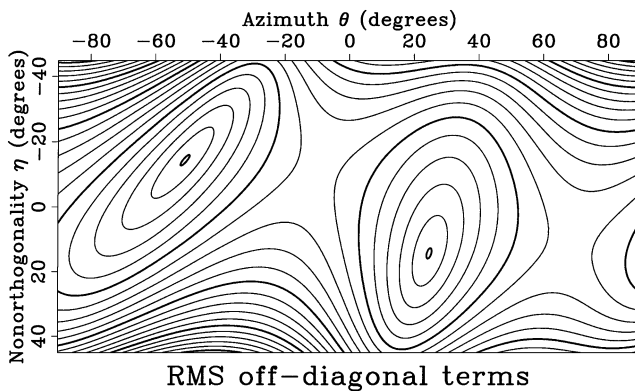


FIG. 6. A contour plot of the rms amplitude of the off-diagonal elements of the data shown in Figure 3 after symmetric Alford diagonalization for a range of trial values of  $\theta$  and  $\eta$ . The function has two minima, both of which correspond to the correct solution.

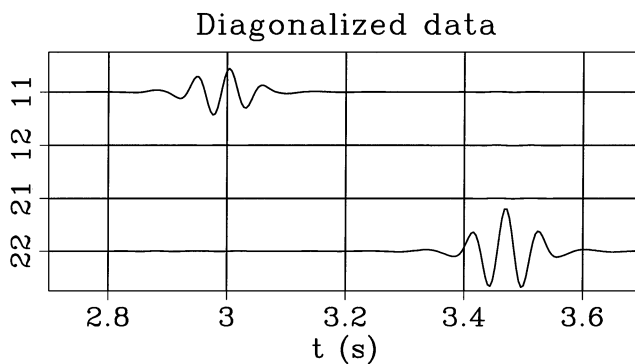


FIG. 7. The data in Figure 3 after symmetric Alford diagonalization, using  $\theta = 24.9^\circ$  (specifying the azimuth of mode 2) and  $\eta = 14.4^\circ$ .

ties of the two shear waves to be resolved. Diagonalization methods that can determine unique modes over short time windows (which include the standard Alford rotation, EED, and SVD methods) do not respect the physics of the nonorthogonal problem.

## DISCUSSION

The EED modeling equation (7) seems intuitive because we habitually use plane waves as a good local approximation for how nonplanar wavefronts behave. A wavefront arriving at a receiver, assuming it does not happen to focus there, can be locally approximated as a plane wave. This is why there is no disagreement in the literature about how to calculate the matrix  $\mathbf{P}_{M \rightarrow R}$ : at the receivers, our intuition works, and we naturally find the correct result. Wavefronts at a focus cannot be modeled as isolated plane waves, however. Not realizing that doing so is invalid is a common source of paradoxes in geophysics (Eisner, 1983; Claerbout and Dellinger, 1987). A point source (by definition, located at a focus) must instead be decomposed linearly into a sum of plane-wave components and each plane-wave component treated separately (Dahlen and Odom, 1984).

### The connection between Alford rotation and ray tracing

Fortunately, equation (1), the general linear modeling equation, is well known in the ray-tracing literature. There it is written

$$R_{j,m}(\omega) = \sum_{n=1}^N P_j^{(n)}(\mathbf{x}_R) D^{(n)}(\omega) P_m^{(n)}(\mathbf{x}_S) \quad (17)$$

where  $N$  is the number of rays from source to receiver,  $P_m^{(n)}(\mathbf{x}_S)$  is component  $m$  of the particle-motion polarization vector associated with raypath number  $n$  at the source location  $\mathbf{x}_S$ ,  $P_j^{(n)}(\mathbf{x}_R)$  is component  $j$  of the particle-motion polarization vector associated with raypath number  $n$  at the receiver location  $\mathbf{x}_R$ , and  $R_{j,m}(\omega)$  is the complex amplitude at frequency  $\omega$  recorded on component  $j$  of the receiver due to an impulse from component  $m$  of the source. The  $D^{(n)}(\omega)$ , one for each ray, contain source and receiver directivity, geometrical spreading, and phase-shift terms multiplied together (Pšenčík and Teles, 1996). In the

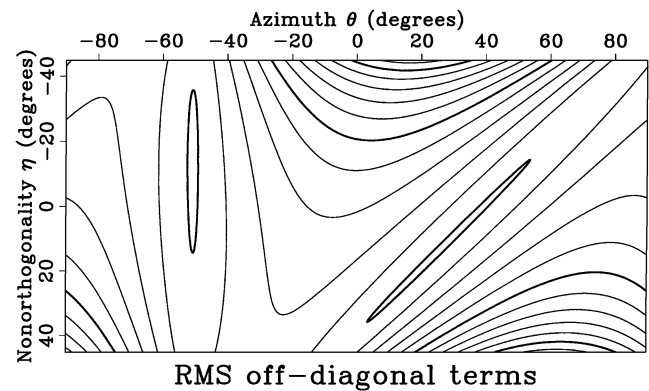


FIG. 8. As Figure 6 but the end of the time window has been advanced to 3.35 s, almost entirely excluding the slow split shear wave. The elongated shape of the minima reflects the lack of information about this event.

ray-tracing literature these scalar terms are traditionally written out separately, obscuring the relationship between equations (17) and (1). Equation (17) holds in the high-frequency limit for a source and receiver embedded in a smoothly varying anisotropic medium (Červený, 1972; Ben-Menahem et al., 1991; Pšenčík and Teles, 1996; Červený, 2000).

Rewritten in the matrix notation customary in the Alford rotation literature, equation (17) becomes

$$\begin{pmatrix} R_{XX} & R_{YX} & R_{ZX} \\ R_{XY} & R_{YY} & R_{ZY} \\ R_{XZ} & R_{YZ} & R_{ZZ} \end{pmatrix} = \begin{pmatrix} P_{1X}(R) & P_{2X}(R) & P_{3X}(R) & \cdots & P_{NX}(R) \\ P_{1Y}(R) & P_{2Y}(R) & P_{3Y}(R) & \cdots & P_{NY}(R) \\ P_{1Z}(R) & P_{2Z}(R) & P_{3Z}(R) & \cdots & P_{NZ}(R) \end{pmatrix} \times \begin{pmatrix} D_1 & 0 & 0 & \cdots & 0 \\ 0 & D_2 & 0 & \cdots & 0 \\ 0 & 0 & D_3 & \cdots & 0 \\ \vdots & \vdots & \vdots & \ddots & \vdots \\ 0 & 0 & 0 & 0 & D_N \end{pmatrix} \times \begin{pmatrix} P_{1X}(S) & P_{1Y}(S) & P_{1Z}(S) \\ P_{2X}(S) & P_{2Y}(S) & P_{2Z}(S) \\ P_{3X}(S) & P_{3Y}(S) & P_{3Z}(S) \\ \vdots & \vdots & \vdots \\ P_{NX}(S) & P_{NY}(S) & P_{NZ}(S) \end{pmatrix}. \quad (18)$$

Comparing equations (17) and (18) with equation (1), we can now see what the matrices in equation (1) represent. In three dimensions,  $\mathbf{P}_{M \rightarrow R}$  has three rows and  $N$  columns, one for each raypath from source to receiver. Each column of  $\mathbf{P}_{M \rightarrow R}$  is a vector giving the normalized particle motion of the corresponding raypath at the receiver ( $R$ ). The matrix  $\mathbf{P}_{S \rightarrow M}$  has the same form as  $\mathbf{P}_{M \rightarrow R}^T$ ; the  $N$  rows of  $\mathbf{P}_{S \rightarrow M}$  give the normalized particle-motion vectors of the rays at the source ( $S$ ). The  $N \times N$  matrix  $\mathbf{D}$  is diagonal, with one diagonal entry per raypath. In the time domain the diagonal elements of  $\mathbf{D}(t)$  become traces, each giving the scalar impulse response for propagation along the corresponding raypath. In the homogeneous case considered in this paper, the polarizations at the source and receiver are the same,  $\mathbf{P}_{S \rightarrow M} = \mathbf{P}_{M \rightarrow R}^T$ , equation (1) specializes to equation (10), and the data matrix is symmetric ( $\mathbf{R} = \mathbf{R}^T$ ). In the general heterogeneous case with source and receiver not at the same location, the polarizations generally are not the same, and we should not expect to find data-matrix symmetry. If the source and receiver are at the same location, the polarizations are trivially the same and data-matrix symmetry is again guaranteed, even in a heterogeneous medium (Knopoff and Gangi, 1959).

For typical crossed-dipole data we do not have the  $Z$  component available for either the source or receiver. It is easy to see in equation (17) that setting the  $Z$  components of the data matrix equal to zero produces the same result as setting the  $Z$  components of the pure-mode polarization vectors equal to

zero. Solving a 3-D problem in two dimensions by ignoring the  $Z$  components, as we did in our example, is thus a valid procedure. If the data window is chosen to encompass only two different arrivals (in our example the data window did not include the  $qP$  arrival), it finds the projection of the 3-D polarization vectors for those two arrivals onto the 2-D ( $X, Y$ ) data plane. Although an additional unknown scalar factor is introduced because the polarization vectors are no longer normalized after projection onto the 2-D data plane, we are already ignoring the other scalar terms in  $\mathbf{D}$  (geometrical spreading and source and receiver directivity), so this is no loss.

As in the standard Alford diagonalization methods, multiple arrivals of the same wave type from the same direction are also not a problem. These arrivals all have the same polarizations and so effectively comprise one long wavelet. However, triplications, quite likely to occur if the modes are seriously nonorthogonal, introduce additional  $qS$  raypaths with distinct polarizations. In that case  $\mathbf{P}_{M \rightarrow R}$  becomes a nonsquare matrix, with more columns than rows, making the processing equation (11) (which requires  $\mathbf{P}_{M \rightarrow R}^{-1}$  to exist) invalid. One solution would be to choose short data windows that encompass at most two distinct source–receiver polarizations each. Failing that, a more sophisticated processing procedure is required.

### Unresolved issues

Alford rotation was originally applied to modeling and processing reflection-seismic data, not crossed-dipole data. Unless the modes fail to couple at the reflector because of some special symmetry of the experimental geometry (as in the traditional Alford model), this will square the number of possible raypaths from source to receiver, causing more raypaths than source and receiver components and again leading to a nonsquare  $\mathbf{P}_{M \rightarrow R}$ . Alternatively, using the two pure-mode polarizations at the source and receiver and allowing for only two raypaths when processing the data leads to a nondiagonal  $\mathbf{D}$ ; the off-diagonal elements contain the converted energy. In that case it may still be possible to infer the polarizations of the pure modes from the data, but a more sophisticated minimization will be required.

Traditional ray theory also does not allow for a source or receiver on a free surface. Although it may be possible to extend ray theory to include this case (Jílek and Červený, 1996), more work remains to be done. (In the traditional Alford model, the complications caused by the free surface are trivial.) Our generalization of standard Alford rotation [given by equations (2) and (6)] applies only to geometries where both the source and receiver are far from the earth’s surface, as in the crossed-dipole geometry. Figure 9 demonstrates that the symmetry of the data matrix in our synthetic model example is broken if a free surface is introduced into the problem, even though the pure modes of the medium are unchanged.

In practice the data matrix recorded by crossed-dipole logging tools is not symmetric. This could be because of mismatched tool components or uneven coupling. Assuming an ideal instrument, it could also be from heterogeneity (the likely explanation) or, more exotically, gyrotropy (Chichinina and Obolentseva, 1998). Gyrotropy is the elastic analog of optically active compounds in organic chemistry; gyrotropic media lack inversion symmetry, so the symmetry argument of Dellinger and Nolte (1996, 1997) does not apply.

Another possible pitfall is our extreme simplification of the crossed-dipole geometry: in deriving our equations, we have ignored the presence of the borehole. Although the symmetry argument of Dellinger and Nolte (1996, 1997) should go through even in the presence of a borehole (so long as the borehole itself displays inversion symmetry), the presence of the borehole could change the correct equations to use for the source and receiver projection matrices. However, because split flexural waves have the same polarizations as the corresponding bulk shear waves (Ellefsen et al., 1991; Sinha et al., 1994), we expect our processing equation should also properly diagonalize split flexural waves.

Is there any practical geophysical application of nonorthogonal diagonalization methods? Although nonorthogonal shear modes occur to some extent for (almost) all media with anisotropy more complex than transverse isotropy (Rudzki, 1911), media such as the one defined in Table 1 that simultaneously display (for some ray directions) both strongly split shear waves and significant deviation from orthogonality must be extremely anisotropic and hence geophysically implausible. If the splitting is allowed to be weak, however, it is relatively easy to construct geophysically plausible examples with a significant degree of nonorthogonality. For example, even a tiny perturbation of transversely isotropic Greenhorn Shale (Jones

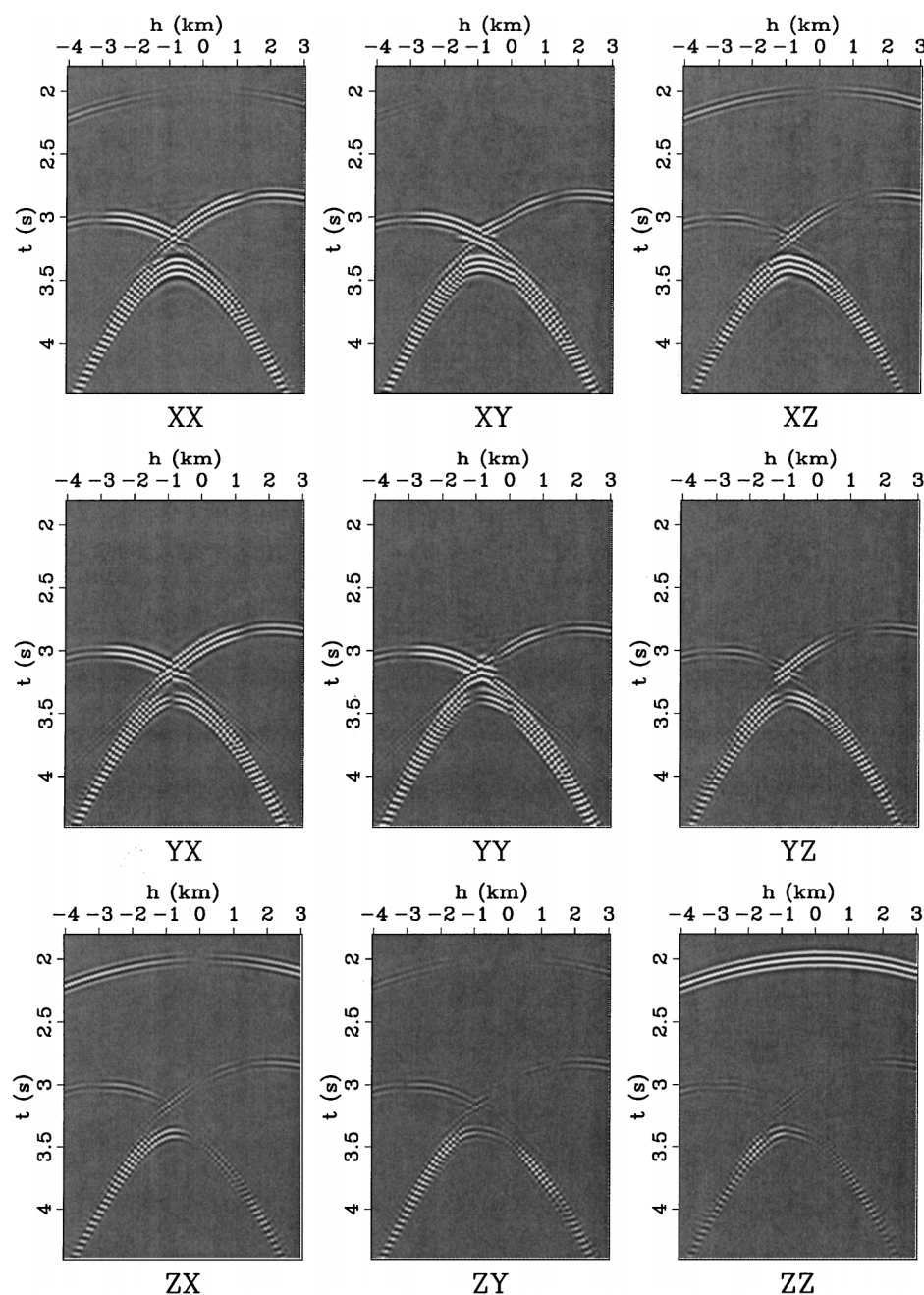


FIG. 9. The same medium and geometry as in Figure 2, but with a free surface located 2 m above the receiver. The data matrix is no longer symmetric.

and Wang, 1981) produces paired connection events with a nonorthogonality approaching 45° (Dellinger, 1991). Recognizing such situations when they do occur in real data will require a processing algorithm that properly accounts for the physics of the problem.

### CONCLUSIONS

We have demonstrated the correct generalized Alford rotation equation for processing crossed-dipole log data. The new method, symmetric Alford diagonalization, allows diagonalization of nonorthogonal shear modes and should be useful for modeling and processing log data recorded in wells not aligned with the symmetry axes of an orthorhombically anisotropic earth.

The idealized homogeneous crossed-dipole geometry examined here is particularly simple because there are no reflections, conversions, or free surfaces to complicate the equations. More work remains to be done to determine the correct generalization of Alford rotation for more general geometries.

### ACKNOWLEDGMENTS

The authors thank Rusty Alford, Leon Thomsen, Paul Gutowski, and Mike Mueller for their accounts of the early history of split shear waves at Amoco and their comments on this work; Jim Brown, whose talk at 7IWSA on reciprocity observed in physical model experiments inspired this paper; Ivan Pšenčík for his guidance in navigating the ray-tracing literature; and Xiang-Yang Li, for his willingness to participate in many useful e-mail discussions.

### REFERENCES

- Alford, R. M., 1986, Shear data in the presence of azimuthal anisotropy: Dilley, Texas: 56th Ann. Internat. Mtg., Soc. Expl. Geophys., Expanded Abstracts, 476–479.
- 1989, Multisource multireceiver method and system for geophysical exploration: U.S. Patent 4 803 666.
- 1991, Method for geophysical exploration: U.S. Patent 5 027 332.
- Auld, B. A., 1973, *Acoustic fields and waves in solids*: Vol. 1: John Wiley & Sons; Inc.
- Ben-Menahem, A., and Sena, A. G., 1990, Seismic source theory in stratified anisotropic media: *J. Geophysical Res.*, **95**, No. B10, 15 395–15 427.
- Ben-Menahem, A., Gibson Jr., R., and Sena, A., 1991, Green's tensor and radiation patterns of point sources in general anisotropic inhomogeneous elastic media: *Geophys. J. Internat.*, **107**, 297–308.
- Buchwald, V. T., 1959, Elastic waves in anisotropic media: *Proc. R. Soc. London, A*, **235**, 563–580.
- Burrige, R., 1967, The singularity on the plane lids of the wave surface of elastic media with cubic symmetry: *Quart. J. Mech. Appl. Math.*, **20**, No. 1, 41–56.
- Červený, V., 1972, Seismic rays and ray intensities in inhomogeneous anisotropic media: *Geophys. J. Roy. Astr. Soc.*, **29**, 1–13.
- 2000, *Seismic ray method*: Cambridge Univ. Press.
- Chichinina, T. I., and Obolentseva, I. R., 1998, Gyrotropy and anisotropy of rocks: Similarities and differences: *Revue de l'Institut Français du Pétrole*, **53**, No. 5, 655–667.
- Claerbout, J. F., and Dellinger, J., 1987, Eisner's reciprocity paradox and its resolution: *The Leading Edge*, **6**, No. 10, 34–37.
- Dahlen, F. A., and Odom, R. I., 1984, Discussion of "Acoustic reciprocity—A paradox": *Geophysics*, **49**, 478–480.
- Dellinger, J., 1991, *Anisotropic seismic wave propagation*: Ph.D. thesis, Stanford Univ.
- Dellinger, J., and Nolte, B., 1996, A cross-dipole reciprocity "paradox": 66th Ann. Internat. Mtg., Soc. Expl. Geophys., Expanded Abstracts, 1223–1226.
- 1997, A crossed-dipole reciprocity "paradox": *The Leading Edge*, **16**, 1465–1471.
- Dellinger, J., Nolte, B., and Etgen, J., 1998, Symmetric Alford diagonalization: 68th Ann. Internat. Mtg., Soc. Expl. Geophys., Expanded Abstracts, 1673–1676.
- Eisner, E., 1983, Acoustic reciprocity—A paradox: *Geophysics*, **48**, 1132–1134.
- Ellefsen, K., Cheng, C., and Toksöz, M., 1991, Applications of perturbation theory to acoustic logging: *J. Geophys. Res.*, **96**, 537–549.
- Esmersoy, C., Koster, K., Williams, M., Boyd, A., and Kane, M., 1994, Dipole shear anisotropy logging: 64th Ann. Internat. Mtg., Soc. Expl. Geophys., Expanded Abstracts, 1139–1142.
- Gajewski, D., 1993, Radiation from point sources in general anisotropic media: *Geophys. J. Internat.*, **113**, 299–317.
- Golub, G. H., and Van Loan, C. F., 1983, *Matrix computations*: Johns Hopkins Univ. Press.
- Hanyga, A., 1984, Point source in anisotropic elastic medium: *Gerlands Beitr. Geophysik*, **93**, No. 6, 463–479.
- Jílek, P., and Červený, V., 1996, Radiation patterns of point sources situated close to structural interfaces and to the earth's surface: *Pure Appl. Geophys.*, **148**, No. 1/2, 175–225.
- Jones, L. E. A., and Wang, H. F., 1981, Ultrasonic velocities in Cretaceous shales from the Williston basin: *Geophysics*, **46**, 288–297.
- Knopoff, L., and Gangi, A. F., 1959, Seismic reciprocity: *Geophysics*, **24**, 681–691.
- Koster, K., Williams, M., Esmersoy, C. E., and Walsh, J. W., 1994, Applied production geophysics using shear-wave anisotropy: Production applications for the dipole shear imager and the multicomponent VSP: 64th Ann. Internat. Mtg., Soc. Expl. Geophys., Expanded Abstracts, 233–235.
- Li, X.-Y., and Crampin, S., 1993, Linear-transform techniques for processing shear-wave anisotropy in four-component seismic data: *Geophysics*, **58**, 240–256.
- Li, X.-Y., MacBeth, C., and Crampin, S., 1998, Interpreting non-orthogonal split shear waves for seismic anisotropy in multicomponent VSPs: *Geophys. Prosp.*, **46**, 1–27.
- Lighthill, M. J., 1960, Studies on magneto-hydrodynamic waves and other anisotropic wave motions: *Phil. Trans. R. Soc. London, A*, **252**, 397–430.
- MacBeth, C., and Crampin, S., 1991, Processing of seismic data in the presence of anisotropy: *Geophysics*, **56**, 1320–1330.
- MacBeth, C., and Li, X.-Y., 1996, Linear matrix operations for multicomponent seismic processing: *Geophys. J. Internat.*, **124**, No. 1, 189–208.
- MacBeth, C., Zeng, X., Yardley, G., and Crampin, S., 1994, Interpreting data matrix asymmetry in near-offset, shear-wave VSP data: *Geophysics*, **59**, 176–191.
- Mallick, S., and Frazer, L. N., 1990, Computation of synthetic seismograms for stratified azimuthally anisotropic media: *J. Geophys. Res.*, **95**, No. B6, 8513–8526.
- Mueller, M. C., Boyd, A. J., and Esmersoy, C., 1994, Case studies of the dipole shear anisotropy log: 64th Ann. Internat. Mtg., Soc. Expl. Geophys. Expanded Abstracts, 1143–1146.
- Murtha, P. E., 1988, Estimation of the rotation transformation angle for shear wave data acquired in azimuthally anisotropic regions: Presented at the 3rd Internat. Workshop on Seismic Anisotropy, Am. Geophys. Union/Soc. Expl. Geophys. Chapman conference.
- Pšenčík, I., and Teles, T. N., 1996, Point source radiation in inhomogeneous anisotropic structures: *Pure Appl. Geophys.*, **148**, 591–623.
- Rudzki, M. P., 1911, *Parametrische Darstellung der elastischen Welle in anisotropen Medien*: Anzeiger der Akademie der Wissenschaften, Krakau, 503–536.
- Sinha, B. K., Norris, A. N., and Chang, S.-K., 1994, Borehole flexural modes in anisotropic formations: *Geophysics*, **59**, 1037–1052.
- Thomsen, L., 1988, Reflection seismology over azimuthally anisotropic media: *Geophysics*, **53**, 304–313.
- Thomsen, L., Tsvankin, I., and Mueller, M. C., 1999, Coarse-layer stripping of vertically variable azimuthal anisotropy from shear-wave data: *Geophysics*, **64**, 1126–1138.
- Tsvankin, I. D., and Chesnokov, E. M., 1990, Synthesis of body wave seismograms from point sources in anisotropic media: *J. Geophys. Res.*, **95**, No. B7, 11 317–11 331.
- Winterstein, D. F., 1990, Velocity anisotropy terminology for geophysicists: *Geophysics*, **55**, 1070–1088.
- 1992, Method of geophysical exploration by analyzing shear-wave polarization directions: U.S. Patent 5 142 501.
- Winterstein, D. F., and Meadows, M. A., 1991, Changes in shear-wave polarization azimuth with depth in Cymric and Railroad Gap oil fields: *Geophysics*, **56**, 1349–1364.
- Zeng, X., and MacBeth, C., 1993, Algebraic processing techniques for estimating shear-wave splitting in near-offset VSP data: *Theory: Geophys. Prosp.*, **41**, 1033–1066.